60 (2015) APPLICATIONS OF MATHEMATICS No. 2, 135–156

APPLICATIONS OF APPROXIMATE GRADIENT SCHEMES FOR NONLINEAR PARABOLIC EQUATIONS

Robert Eymard, Paris, Angela Handlovičová, Bratislava,
Raphaèle Herbin, Marseille, Karol Mikula, Olga Stašová, Bratislava

(Received April 24, 2013)

Abstract. We develop gradient schemes for the approximation of the Perona-Malik equations and nonlinear tensor-diffusion equations. We prove the convergence of these methods to the weak solutions of the corresponding nonlinear PDEs. A particular gradient scheme on rectangular meshes is then studied numerically with respect to experimental order of convergence which shows its second order accuracy. We present also numerical experiments related to image filtering by time-delayed Perona-Malik and tensor diffusion equations.

Keywords: regularized Perona-Malik equation; gradient schemes

MSC 2010: 65M08, 65M12

1. Introduction

A large class of image processing methods is based on the use of approximate solutions to equations of the following type:

$$u_t - \operatorname{div}(G(u,x,t)\nabla u) = r(x,t) \quad \text{for a.e. } (x,t) \in \Omega \times (0,T) \tag{1.1}$$

with the initial condition

$$u(x,0) = u_{\mathrm{ini}}(x) \quad \text{for a.e. } x \in \Omega, \tag{1.2}$$

and homogeneous Neumann boundary condition

$$G(u,x,t)\nabla u(x,t) \cdot \mathbf{n}_{\partial\Omega}(x) = 0 \quad \text{for a.e. } (x,t) \in \partial\Omega \times \mathbb{R}_+, \tag{1.3}$$

The research of A. Handlovičová, K. Mikula and O. Stašová has been supported by grants APVV-0184-10, VEGA 1/1063/11 and VEGA 1/1137/12.

where the following hypotheses, called Hypotheses (H) in this paper, are considered:

- ▷ Ω is an open bounded polyhedron in $\mathbb{R}^d$, $d \in \mathbb{N}^\star$, with boundary $\partial\Omega$,
- ▷ $T > 0$, $u_{\text{ini}} \in L^2(\Omega)$, $r \in L^2(\Omega \times (0,T))$,
- ▷ the possibly nonlocal function G is such that:

$$
\begin{aligned}
&G\colon\ L^2(\Omega) \times \Omega \times (0,T) \to \mathcal{L}(\mathbb{R}^d, \mathbb{R}^d),\\
&G(\cdot, x, t) \text{ is continuous for a.e. } (x,t) \in \Omega \times (0,T),\\
&G(u, \cdot, \cdot) \text{ is measurable for all } u \in L^2(\Omega),\\
&G(u,x,t) \text{ is self-adjoint with eigenvalues in } (\underline{\lambda}, \overline{\lambda}),\ \underline{\lambda} > 0\\
&\text{for all } u \in L^2(\Omega) \text{ and for a.e. } (x,t) \in \Omega \times (0,T),
\end{aligned}
\tag{1.4}
$$

denoting by $\mathcal{L}(\mathbb{R}^d, \mathbb{R}^d)$ the set of linear mappings from $\mathbb{R}^d$ to $\mathbb{R}^d$.

In image processing applications, u_{ini} represents an original noisy image, the solution $u(x,t)$ represents its filtering which depends on the scale parameter t. The space dimension d is equal to 2 for 2D image filtering, 3 for 3D image or 2D+time movie filtering and 4 for 3D+time filtering of spatio-temporal image sequences. The image processing methods based on approximations of equation (1.1) differ by the definition of the function G. In this paper, we consider cases where G arises from some regularization of the Perona-Malik equation [20], which reads

$$\partial_t u - \operatorname{div}(g(|\nabla u|)\nabla u) = 0, \tag{1.5}$$

where

$$g(s) = \frac{1}{1 + K s^2} \quad \forall\, s \in \mathbb{R}^+, \tag{1.6}$$

for a given $K > 0$. Recall that the mapping $s \mapsto sg(s)$ is not monotonically increasing on $\mathbb{R}^+$, and therefore the Perona-Malik equation is an ill-posed parabolic problem on general initial data.

The convergence of a numerical scheme for the one-dimensional original Perona-Malik problem (1.5) is proved in [4]. The analysis of a finite element discretization of a modified Perona-Malik equation is performed in [3]; in this latter work, the function g depends on the x and y derivatives of u, rather than on the norm of the full gradient, which is the case considered here.

We first consider a regularization of the example due to Catté, Lions, Morel, and Coll [6]; this example gives an approximation of the time delayed Perona-Malik equation, using

$$\partial_t u - \operatorname{div}(G(u(\cdot,t),\cdot)\nabla u) = 0 \tag{1.7}$$

with

$$G(u,x) = \max\left(g\left(\left|\int_\Omega u(y)\nabla G_\sigma(x-y)\,\mathrm{d}y\right|\right),\alpha\right) \quad \forall\, u \in L^1(\Omega), \tag{1.8}$$

where $\alpha > 0$ is a given small value (in [6], although the parameter α is not introduced, a similar bound as below is obtained) and $G_\sigma \in C^\infty(\mathbb{R}^d)$ is a smoothing kernel, e.g., the Gauss function or mollifier with a compact support, for which $\int_{\mathbb{R}^d} G_\sigma(x)\,\mathrm{d}x = 1$. Thanks to the convolution properties, the nonlinearity in the diffusion term depends on the unknown function u, contrary to the original Perona-Malik equation (without convolution) where it depends on the gradient of the solution. Note that since the function $s \mapsto \max(g(s),\alpha)$ is Lipschitz continuous with some constant L_g, we get that for all $u, v \in L^1(\Omega)$,

$$\begin{aligned}|G(u,x) - G(v,x)| &\leqslant L_g\left|\left|\int_\Omega u(y)\nabla G_\sigma(x-y)\,\mathrm{d}y\right| - \left|\int_\Omega v(y)\nabla G_\sigma(x-y)\,\mathrm{d}x\right|\right| \\ &\leqslant L_g\left|\int_\Omega (u(y)-v(y))\nabla G_\sigma(x-y)\,\mathrm{d}y\right| \leqslant L_g\|\nabla G_\sigma\|_\infty\|u-v\|_{L^1(\Omega)},\end{aligned}$$

which shows that (1.8) enters into the framework defined by Hypotheses (H). In the case of the regularized model, the convergence of classical finite volume schemes was proved in [19], [17].

Another interesting image processing model with the structure of equation (1.1) is the so-called nonlinear tensor anisotropic diffusion introduced by Weickert [21]. In that case, the linear mapping $G(u,x,t)$ represents the so-called diffusion tensor depending on the eigenvalues and eigenvectors of the (regularized) structure tensor with matrix

$$J_\varrho(\nabla u_\sigma) = G_\varrho * (\nabla u_\sigma \nabla u_\sigma{}^{\mathrm{T}}), \tag{1.9}$$

where $f * g$ denotes the convolution between the two functions f and g, u_σ is defined by

$$u_\sigma(x,t) = (G_\sigma * u(\cdot,t))(x) \tag{1.10}$$

and G_σ and G_ϱ are Gaussian kernels. In computer vision, the matrix $J_\varrho = \left(\begin{smallmatrix} a & b \\ b & c \end{smallmatrix}\right)$, which is symmetric and positive semidefinite, is also known as the interest operator or second moment matrix. We may write $a = G_\varrho * (\partial_1 G_\sigma * u)^2$, $b = G_\varrho * ((\partial_1 G_\sigma * u)(\partial_2 G_\sigma * u))$ and $c = G_\varrho * (\partial_2 G_\sigma * u)^2$. The orthogonal set of eigenvectors (v,w) of J_ϱ corresponding to its eigenvalues (μ_1,μ_2), $\mu_1 \geqslant \mu_2$, is such that the orientation of the eigenvector w, which corresponds to the smaller eigenvalue μ_2, gives

the so-called coherence orientation. This orientation has the lowest fluctuations in image intensity. The diffusion tensor G in equation (1.1) is then designed to steer a smoothing process so that the filtering is strong along the coherence direction w and increasing with the coherence defined by the difference of the eigenvalues $(\mu_1 - \mu_2)^2$. To that goal, G must possess the same eigenvectors $v = (v_1, v_2)$ and $w = (-v_2, v_1)$ as the structure tensor $J_\varrho(\nabla u_\sigma)$ and the eigenvalues of G can be chosen as follows:

$$\kappa_1 = \alpha, \quad \alpha \in (0,1),\ \alpha \ll 1, \tag{1.11}$$
$$\kappa_2 = \begin{cases} \alpha, & \text{if } \mu_1 = \mu_2, \\ \alpha + (1-\alpha)\exp\Big(\dfrac{-C}{(\mu_1-\mu_2)^2}\Big),\ C > 0 & \text{otherwise.} \end{cases}$$

So, the matrix M_G of the linear operator $G(u, x, t)$ is finally defined by

$$M_G = ABA^{-1}, \quad \text{where } A = \begin{pmatrix} v_1 & -v_2 \\ v_2 & v_1 \end{pmatrix} \text{ and } B = \begin{pmatrix} \kappa_1 & 0 \\ 0 & \kappa_2 \end{pmatrix}. \tag{1.12}$$

Thanks to this construction by convolutions, the diffusion matrix (nonlinearly) depends on the solution u and it satisfies smoothness, symmetry and uniform positive definiteness properties. It is then possible to show that it enters into Hypotheses (H) by similar computations to those done above and in [9]. The so-called diamond-cell finite volume schemes for the nonlinear tensor anisotropic diffusion were suggested and analyzed in [9], [8].

Another type of regularization of the classical Perona-Malik approach is obtained by considering the gradient information from delayed time $t - \overline{t}$, for a given $\overline{t} > 0$. We call this model the time-delayed Perona-Malik equation: consider (1.1) with $u_{\text{ini}} \in H^1(\Omega)$, and define $u(x,t) = u_{\text{ini}}(x)$ for $x \in \Omega$ and $t < 0$. Then, for any $k \in \mathbb{N}$, we define the function G in the time interval $(k\overline{t}, (k+1)\overline{t})$, by

$$G(x,t) = \max(g(|\nabla u(x, t-\overline{t})|), \alpha), \tag{1.13}$$

where $\alpha > 0$ is again a small parameter. Then problem (1.1) boils down to a standard linear parabolic problem on $(k\overline{t}, (k+1)\overline{t})$ (which is included in the framework of Hypotheses (H)), and, as shown in the numerical part of this paper, it leads to an efficient approximation of the Perona-Malik equation.

An integral average on a given shifted time interval is used in [2] for regularization purposes. Our regularization can be understood as a discrete approximation of the integral average, e.g., by a mid-point rule. Note that the Amann theory holds for the original integral regularization without numerical integration while our theory and convergence proofs are valid for the gradient approximation shifted backward in time.

We focus in this paper on the use of the family of gradient schemes [14], [13] for the approximation of the preceding problems. Indeed, this general framework simultaneously includes conforming finite element methods, with or without mass lumping, mixed finite elements, nonconforming P^1 finite elements, and a large variety of more recent methods inspired by finite volume schemes (in particular the Hybrid Mimetic Mixed family which includes the Mimetic Finite Difference schemes, the SUSHI scheme and the Mixed Finite Volume scheme, see [10]). The particular gradient scheme which is used in this paper can be seen as a Multi-Point Flux-Approximation scheme [1]. The interest of directly studying the convergence of the family of gradient schemes is that the proofs which are done here apply to the whole family of discretizations entering into this framework.

This paper is organized as follows. After providing the description of a weak solution in Section 2, we define the class of gradient schemes for the approximation of models based on equation (1.1). We then prove their convergence in Section 3. Then in Section 4, we consider a particular scheme applied to the approximation of the time-delayed Perona-Malik equation and nonlinear tensor-diffusion equation for image filtering purposes. Finally, numerical results are presented in Section 5, exhibiting the accuracy of the proposed method and original applications to image filtering.

2. The weak formulation

Definition 2.1 (Weak solution to (1.1)–(1.3))**.** Under Hypotheses (H), a function u is a weak solution of (1.1)–(1.3) if, for all $T > 0$,

(1) $u \in L^2(0,T;H^1(\Omega))$,
(2) the following holds:

$$\begin{aligned}(2.1)\qquad &\int_0^T\int_\Omega (-u(x,t)\varphi_t(t)w(x) + \varphi(t)G(u,x,t)\nabla u(x,t)\cdot\nabla w(x))\,\mathrm{d}x\,\mathrm{d}t \\ &\quad - \int_\Omega u_{\mathrm{ini}}(x)w(x)\varphi(0)\,\mathrm{d}x = \int_0^T\int_\Omega r(x,t)w(x)\varphi(t)\,\mathrm{d}x\,\mathrm{d}t \\ &\qquad\qquad \forall\, w\in H^1(\Omega),\ \forall\,\varphi\in C_c^\infty([0,T)),\end{aligned}$$

where we denote by $C_c^\infty([0,T))$ the set of functions of $C_c^\infty((-\infty,T))$ restricted to $[0,T)$.

We have the following standard result [5].

Theorem 2.1 (Properties of a weak solution u to (1.1)–(1.3))**.** *Under Hypotheses* (H)*, the function u is a weak solution to* (1.1)–(1.3) *in the sense of Definition* 2.1 *if and only if*

(1) $u \in L^2(0,T;H^1(\Omega))$, $u_t \in L^2(0,T;H^1(\Omega)')$ (*defining the standard continuous embedding of $L^2(\Omega)$ in $H^1(\Omega)'$), and therefore $u \in C^0([0,T];L^2(\Omega))$,*

(2) $u(x,0) = u_{\mathrm{ini}}(x)$ *for a.e.* $x \in \Omega$,

(3) *the following holds:*

$$\int_0^T \Big(\langle u_t(t), v(t) \rangle_{H^1(\Omega)',H^1(\Omega)} + \int_\Omega G(u,x,t) \nabla u(x,t) \cdot \nabla v(x,t) \,\mathrm{d}x \Big) \,\mathrm{d}t = \int_0^T \int_\Omega r(x,t) v(x,t) \,\mathrm{d}x \,\mathrm{d}t \quad \forall\, v \in L^2(0,T;H^1(\Omega)). \tag{2.2}$$

Then u satisfies the following consequence of the above properties:

$$\frac{1}{2} \int_\Omega (u(x,t_0)^2 - u_{\mathrm{ini}}(x)^2) \,\mathrm{d}x + \int_0^{t_0} \int_\Omega G(u,x,t) \nabla u(x,t) \cdot \nabla u(x,t) \,\mathrm{d}x \,\mathrm{d}t = \int_0^{t_0} \int_\Omega r(x,t) u(x,t) \,\mathrm{d}x \,\mathrm{d}t \quad \forall\, t_0 \in [0,T]. \tag{2.3}$$

3. Approximate gradient schemes for parabolic equations

3.1. Definition of the scheme

Definition 3.1 (Approximate gradient discretization and gradient scheme)**.** Under Hypotheses (H), an *approximate gradient discretization* $\mathcal{D}$ is defined by $\mathcal{D} = (X_\mathcal{D}, \Pi_\mathcal{D}, \nabla_\mathcal{D})$, where:

(1) the set of discrete unknowns $X_\mathcal{D}$ is a finite dimensional vector space on $\mathbb{R}$,

(2) the mapping $\Pi_\mathcal{D} \colon X_\mathcal{D} \to L^2(\Omega)$ is the reconstruction of the approximate function,

(3) the mapping $\nabla_\mathcal{D} \colon X_\mathcal{D} \to L^2(\Omega)^d$ is the reconstruction of the gradient of the function,

(4) $\|u\|_\mathcal{D} = \big(\|\Pi_\mathcal{D} u\|_{L^2(\Omega)}^2 + \|\nabla_\mathcal{D} u\|_{L^2(\Omega)^d}^2 \big)^{1/2}$ is a norm on $X_\mathcal{D}$.

Then the *compactness* of the discretization is measured by the function $T_\mathcal{D} \colon \mathbb{R}^d \to \mathbb{R}^+$, defined by

$$T_\mathcal{D}(\xi) = \max_{v \in X_\mathcal{D} \setminus \{0\}} \frac{\|\Pi_\mathcal{D} v(\cdot + \xi) - \Pi_\mathcal{D} v\|_{L^2(\mathbb{R}^d)}}{\|v\|_\mathcal{D}} \quad \forall\, \xi \in \mathbb{R}^d, \tag{3.1}$$

where $\Pi_\mathcal{D} v$ is set to zero outside of Ω. Note that $\lim_{|\xi| \to 0} T_\mathcal{D}(\xi) = 0$.

The *strong consistency* of the discretization is measured by the interpolation error function $S_{\mathcal{D}}\colon H_0^1(\Omega) \to [0,\infty)$, defined by

$$S_{\mathcal{D}}(\varphi) = \min_{v\in X_{\mathcal{D}}} (\|\Pi_{\mathcal{D}} v - \varphi\|_{L^2(\Omega)}^2 + \|\nabla_{\mathcal{D}} v - \nabla\varphi\|_{L^2(\Omega)^d}^2)^{1/2} \quad \forall\, \varphi \in H^1(\Omega). \tag{3.2}$$

The *limit conformity* of the discretization is measured by the conformity error function $W_{\mathcal{D}}\colon H_{\mathrm{div},0}(\Omega) \to [0,+\infty)$ (where $H_{\mathrm{div},0}(\Omega)$ denotes the set of all elements of $H_{\mathrm{div}}(\Omega)$ with zero normal trace), defined by

$$W_{\mathcal{D}}(\boldsymbol{\varphi}) = \max_{u\in X_{\mathcal{D}}\setminus\{0\}} \frac{1}{\|u\|_{\mathcal{D}}} \left| \int_\Omega (\nabla_{\mathcal{D}} u(\boldsymbol{x}) \cdot \boldsymbol{\varphi}(\boldsymbol{x}) + \Pi_{\mathcal{D}} u(\boldsymbol{x}) \operatorname{div} \boldsymbol{\varphi}(\boldsymbol{x}))\, \mathrm{d}\boldsymbol{x} \right| \quad \forall \boldsymbol{\varphi} \in H_{\mathrm{div},0}(\Omega). \tag{3.3}$$

Definition 3.2 (Space-time discretization)**.** Let the Hypotheses (H) be fulfilled. We say that $(\mathcal{D},\tau)$ is a *space-time gradient discretization* of $\Omega\times(0,T)$, if

- $\mathcal{D} = (X_{\mathcal{D}}, \Pi_{\mathcal{D}}, \nabla_{\mathcal{D}})$ is an approximate gradient discretization of Ω in the sense of Definition 3.1,
- there exists $N_T \in \mathbb{N}$ with $T = N_T\tau$, where $\tau > 0$ is the time step.

We then define $X_{\mathcal{D},\tau} = \{(u^n)_{n=1,\dots,N_T}, u^n \in X_{\mathcal{D}}\}$, and we define the mappings $\Pi_{\mathcal{D},\tau}\colon X_{\mathcal{D},\tau} \to L^2(\Omega\times(0,T))$ and $\nabla_{\mathcal{D},\tau}\colon X_{\mathcal{D},\tau} \to L^2(\Omega\times(0,T))^d$ by

$$\Pi_{\mathcal{D},\tau} u(x,t) = \Pi_{\mathcal{D}} u^n(x) \text{ for a.e. } x\in\Omega,\ \forall\, t\in((n-1)\tau, n\tau],\ \forall\, n = 1,\dots,N_T, \tag{3.4}$$

and

$$\nabla_{\mathcal{D},\tau} u(x,t) = \nabla_{\mathcal{D}} u^n(x) \text{ for a.e. } x\in\Omega,\ \forall\, t\in((n-1)\tau, n\tau],\ \forall\, n = 1,\dots,N_T. \tag{3.5}$$

Let $(\mathcal{D},\tau)$ be a space-time discretization of $\Omega\times(0,T)$. We define the following scheme for the discretization of problem (1.1):

$$\begin{aligned} u \in X_{\mathcal{D},\tau},\ \delta_\tau u(x,t) &= \frac{1}{\tau}(\Pi_{\mathcal{D}} u^1(x) - u_{\mathrm{ini}}(x)) \quad \text{for a.e. } x\in\Omega,\ \forall\, t\in(0,\tau], \\ \delta_\tau u(x,t) &= \frac{1}{\tau}(\Pi_{\mathcal{D}} u^n(x) - \Pi_{\mathcal{D}} u^{n-1}(x)) \quad \text{for a.e. } x\in\Omega, \\ &\qquad \forall\, t\in((n-1)\tau, n\tau],\ \forall\, n = 2,\dots,N_T, \end{aligned} \tag{3.6}$$

and

$$\begin{aligned} &\int_0^T \int_\Omega (\delta_\tau u\, \Pi_{\mathcal{D},\tau} v + G_{\mathcal{D},\tau}(\Pi_{\mathcal{D},\tau} u, x, t) \nabla_{\mathcal{D},\tau} u \cdot \nabla_{\mathcal{D},\tau} v)\, \mathrm{d}x\, \mathrm{d}t \\ &\qquad = \int_0^T \int_\Omega r \Pi_{\mathcal{D},\tau} v\, \mathrm{d}x\, \mathrm{d}t, \quad \forall\, v \in X_{\mathcal{D},\tau}, \end{aligned} \tag{3.7}$$

where

$$
\begin{aligned}
(3.8)\qquad & G_{\mathcal{D},\tau}\colon\ L^2(\Omega)\times\Omega\times(0,T)\to\mathcal{L}(\mathbb{R}^d,\mathbb{R}^d),\ \text{there exists } C_{\mathcal{D},\tau}>0\\
& \text{with } \|G_{\mathcal{D},\tau}(v,x,t)-G(v,x,t)\|_{\mathcal{L}(\mathbb{R}^d,\mathbb{R}^d)}\leqslant C_{\mathcal{D},\tau}\|v\|_{L^2(\Omega)},\\
& \forall\, v\in L^2(\Omega),\ \text{for a.e. } (x,t)\in\Omega\times(0,T),\\
& G_{\mathcal{D},\tau}(u,\cdot,\cdot)\ \text{is measurable for all } u\in L^2(\Omega\times(0,T)),\\
& G_{\mathcal{D},\tau}(u,x,t)\ \text{is self-adjoint with eigenvalues in } (\underline{\lambda},\overline{\lambda})\\
& \text{for all } u\in L^2(\Omega) \text{ and for a.e. } (x,t)\in\Omega\times(0,T).
\end{aligned}
$$

We then denote $\Pi_{\mathcal{D},\tau}u(\cdot,0)=u_{\rm ini}$, hence defining $\Pi_{\mathcal{D},\tau}u(\cdot,t)$ for all $t\in[0,T]$.

R e m a r k 3.1. Note that assumption (3.8) holds in particular for $G_{\mathcal{D},\tau}=G$, which occurs in some of the numerical applications.

3.2. Properties of the scheme

Lemma 3.1 ($L^\infty(0,T;L^2(\Omega))$ and $L^2(0,T;H^1(\Omega))$ estimates and existence of a discrete solution)**.** *Under Hypotheses* (H)*, let* $(\mathcal{D},\tau)$ *be a space-time gradient discretization of* $\Omega\times(0,T)$ *in the sense of Definition* 3.2*. Then there exists at least one solution to scheme* (3.6)–(3.7)*, which moreover satisfies that there exists a constant* $C_1>0$ *such that*

$$
(3.9)\qquad \|\Pi_{\mathcal{D}}u^m\|^2_{L^2(\Omega)}\leqslant C_1(\|u_{\rm ini}\|^2_{L^2(\Omega)}+T\|r\|^2_{L^2(\Omega\times(0,T))})\quad\forall\, m=1,\dots,N_T,
$$

and

$$
(3.10)\qquad \|\nabla_{\mathcal{D},\tau}u\|^2_{L^2(\Omega\times(0,T))^d}\leqslant\frac{C_1}{\underline{\lambda}}(\|u_{\rm ini}\|^2_{L^2(\Omega)}+T\|r\|^2_{L^2(\Omega\times(0,T))}).
$$

P r o o f. Let $m=1,\dots,N_T$ and let us set $v^n=u^n$ for $n=1,\dots,m$ and $v^n=0$ for $n=m+1,\dots,N_T$ in (3.7). We obtain, thanks to the equality $a(a-b)=\frac12(a^2+(a-b)^2-b^2)$,

$$
\begin{aligned}
(3.11)\qquad \int_\Omega\left(\frac12(\Pi_{\mathcal{D}}u^m(x)^2-u_{\rm ini}(x)^2)+\underline{\lambda}\int_0^{m\tau}|\nabla_{\mathcal{D},\tau}u(x,t)|^2\,{\rm d}t\right){\rm d}x&\\
\leqslant\int_0^{m\tau}\int_\Omega r(x,t)\Pi_{\mathcal{D},\tau}u(x,t)\,{\rm d}x\,{\rm d}t.&
\end{aligned}
$$

Applying the Young inequality to the right-hand side provides

$$
\begin{aligned}
&\int_\Omega\left(\frac12(\Pi_{\mathcal{D}}u^m(x)^2-u_{\rm ini}(x)^2)+\underline{\lambda}\int_0^{m\tau}|\nabla_{\mathcal{D},\tau}u(x,t)|^2\,{\rm d}t\right){\rm d}x\\
&\qquad\leqslant T\int_0^{m\tau}\int_\Omega r(x,t)^2\,{\rm d}x\,{\rm d}t+\frac{1}{4T}\int_0^{m\tau}\int_\Omega\Pi_{\mathcal{D},\tau}u(x,t)^2\,{\rm d}x\,{\rm d}t.
\end{aligned}
$$

We now give a discrete version of the Gronwall lemma. For $a_m = \int_\Omega \Pi_{\mathcal{D}} u^m(x)^2 \,\mathrm{d}x$, $b = \int_\Omega u_{\mathrm{ini}}(x)^2 \,\mathrm{d}x + 2T \int_0^T \int_\Omega r(x,t)^2 \,\mathrm{d}x \,\mathrm{d}t$, we get

$$a_m \leqslant b + \frac{1}{2T} d_m \quad \text{with } d_m = \tau \sum_{n=1}^{m} a_n,$$

which can be written, setting $c = \tau/2T \leqslant 1/2$ and $d_0 = 0$, as

$$d_m - d_{m-1} \leqslant \tau b + c d_m.$$

This gives $d_m \leqslant (d_{m-1} + \tau b)/(1-c)$, and therefore $d_m \leqslant \tau \sum_{n=1}^{m} b/(1-c)^{m+1-n}$. Using the inequality $mc \leqslant 1/2$, which leads to $-\log(1-c) \leqslant \log(2m/(2m-1))$, we get

$$\log \frac{1}{(1-c)^m} \leqslant m \log \frac{2m}{2m-1} \leqslant m\Big(\frac{2m}{2m-1} - 1\Big) = \frac{m}{2m-1} \leqslant 1,$$

and therefore $1/(1-c)^m \leqslant \mathrm{e}$. We have

$$\tau \sum_{n=1}^{m} \frac{1}{(1-c)^{m+1-n}} \leqslant \tau \frac{1/(1-c)^{m+1} - 1}{1/(1-c) - 1} \leqslant \frac{\tau}{\tau/2T} \frac{1}{(1-c)^m} \leqslant 2T\mathrm{e},$$

which gives $d_m \leqslant 2T\mathrm{e}b$. Hence, we conclude $a_m \leqslant (1 + 2\mathrm{e})b$, which yields (3.9) and (3.10). The topological degree argument applied to numerical schemes (see, e.g., [15]) allows to conclude to the existence of at least one solution to the scheme. □

Note that the minimal regularity of the initial data corresponding to the framework of image processing, and the generality of the operator G prevent from obtaining more regular estimates than those of Lemma 3.1. In particular, multiplying the scheme with a discrete time derivative does not seem to yield a better estimate.

We may now state the convergence theorem.

Theorem 3.1. *Let Hypotheses* (H) *be fulfilled. Let* $(\mathcal{D}_m, \tau_m)_{m\in\mathbb{N}}$ *be a sequence of space-time discretizations of* $\Omega \times (0,T)$ *in the sense of Definition* 3.2 *such that* $C_{\mathcal{D}_m,\tau_m}$ *(introduced in* (3.8)*) and* $\tau_m > 0$ *tend to* 0 *as* $m \to \infty$. *We assume that there exists a function* $\widetilde{T}\colon \mathbb{R}^d \to \mathbb{R}^+$ *with* $\lim_{|\xi|\to 0} \widetilde{T}(\xi) = 0$ *such that* $T_{\mathcal{D}_m} \leqslant \widetilde{T}$ *for all* $m \in \mathbb{N}$, *and that*

$$\forall\, \varphi \in H^1(\Omega),\ \lim_{m\to\infty} S_{\mathcal{D}_m}(\varphi) = 0, \tag{3.12}$$

and

$$\forall\, \boldsymbol{\varphi} \in H_{\mathrm{div},0}(\Omega),\ \lim_{m\to\infty} W_{\mathcal{D}_m}(\boldsymbol{\varphi}) = 0. \tag{3.13}$$

Let, for all $m \in \mathbb{N}$, $u_m \in X_{\mathcal{D}_m,\tau_m}$ *be such that* (3.6)–(3.7) *hold.*

Then there exists a weak solution u to (1.1)–(1.3) in the sense of Definition 2.1 such that, up to a subsequence, $\Pi_{\mathcal{D}_m,\tau_m} u_m$ tends to u in $L^2(\Omega\times(0,T))$, and $\nabla_{\mathcal{D}_m} u_{\mathcal{D}_m,\tau_m}$ tends to ∇u for the weak topology of $L^2(\Omega\times(0,T))^d$. In the case that u is unique, the whole sequence converges in the same sense.

P r o o f. Thanks to (3.9)–(3.10), we have the existence of some $C_2>0$, independent of m, such that

$$\|\Pi_{\mathcal{D}_m,\tau_m} u_m(\cdot+\xi,\cdot)-\Pi_{\mathcal{D}_m,\tau_m} u_m\|_{L^2(\mathbb{R}^d\times(0,T)}\leqslant C_2\widetilde{T}(\xi).$$

Let us now prove an estimate on the time translates. Let $\eta\in(0,T)$. We drop the index m for the simplicity of notation. We consider

$$A(\eta)=\|\Pi_{\mathcal{D},\tau}u(\cdot,\cdot+\eta)-\Pi_{\mathcal{D},\tau}u\|^2_{L^2(\Omega\times(0,T-\eta))}.$$

Denoting by $\nu(t)$ the integer n such that $t\in((n-1)\tau,n\tau]$, we have $A(\eta)=\int_0^{T-\eta}\sum_{n=\nu(t)}^{\nu(t+\eta)}\tau(A_1^n-A_2^n)\,\mathrm{d}t$, with

$$A_1^n=\frac{1}{\tau}\int_\Omega(\Pi_{\mathcal{D},\tau}u^n-\Pi_{\mathcal{D},\tau}u^{n-1})\Pi_{\mathcal{D}}u^{\nu(t+\eta)}\,\mathrm{d}x$$

and

$$A_2^n=\frac{1}{\tau}\int_\Omega(\Pi_{\mathcal{D},\tau}u^n-\Pi_{\mathcal{D},\tau}u^{n-1})\Pi_{\mathcal{D}}u^{\nu(t)}\,\mathrm{d}x.$$

Using (3.7) with $v^n=u^{\nu(t+\eta)}$ and $v^p=0$ for $p\neq n$, we get

$$\begin{aligned}A_1^n=\frac{1}{\tau}\int_{(n-1)\tau}^{n\tau}\int_\Omega&(r(x,s)\Pi_{\mathcal{D},\tau}u^{\nu(t+\eta)}(x)\\&-G_{\mathcal{D},\tau}(\Pi_{\mathcal{D},\tau}u,x,s)\nabla_{\mathcal{D}}u^n(x)\cdot\nabla_{\mathcal{D}}u^{\nu(t+\eta)}(x))\,\mathrm{d}x\,\mathrm{d}s.\end{aligned}$$

Thus, we obtain applying Young's inequality that

$$A_1^n\leqslant\frac{1}{2}(A_{11}^n+A_{12}^{\nu(t+\eta)}+A_{13}^n+A_{13}^{\nu(t+\eta)}),$$

with

$$A_{11}^n=\frac{1}{\tau}\int_{(n-1)\tau}^{n\tau}\int_\Omega r(x,s)^2\,\mathrm{d}x\,\mathrm{d}s,\ A_{12}^n=\int_\Omega(\Pi_{\mathcal{D},\tau}u^n)^2\,\mathrm{d}x,\ A_{13}^n=\overline{\lambda}\int_\Omega(\nabla_{\mathcal{D}}u^n)^2\,\mathrm{d}x.$$

A similar inequality holds for A_2^n. Hence, using Lemma 6.1 stated in the Appendix, and (3.9)–(3.10), we get the existence of C_3, which does not depend on m, such that

$$A(\eta)\leqslant C_3\eta.$$

Thanks to (3.9) which is a $L^\infty(0,T;L^2(\Omega))$ bound on the approximate solution, it is easy to extend the time translates from $(0,T-\eta)$ to $\mathbb{R}$, for the approximate solution set to 0 outside of $\Omega\times(0,T)$. This proves that the time translates of $\Pi_{\mathcal{D}_m,\tau_m}u_m$ uniformly tend to 0. Then, thanks to Kolmogorov's theorem, we may extract a subsequence such that $\Pi_{\mathcal{D}_m,\tau_m}u_m$ converges in $L^2(\Omega\times(0,T))$ to some function $u\in L^2(\Omega\times(0,T))$. Since $\nabla_{\mathcal{D}_m,\tau_m}u_m$ is bounded in $L^2(\Omega\times(0,T))^d$, it weakly converges in $L^2(\Omega\times(0,T))^d$, up to a subsequence, to some function $\widetilde{G}$. For given $\boldsymbol{\varphi}\in H_{\mathrm{div},0}(\Omega)$ and $\varphi\in C_c^\infty((0,T))$, we can write, using (3.3),

$$t\left|\int_0^T\int_\Omega \varphi(t)(\nabla_{\mathcal{D}_m,\tau_m}u_m\cdot\boldsymbol{\varphi}+\Pi_{\mathcal{D}_m,\tau_m}u_m\ \operatorname{div}\boldsymbol{\varphi})\,\mathrm{d}x\,\mathrm{d}t\right| \leqslant \int_0^T W_{\mathcal{D}_m}(\boldsymbol{\varphi})\varphi(t)\|u_m(t)\|_{\mathcal{D}_m}\,\mathrm{d}t.$$

Letting $m\to\infty$ in the above inequality (which is possible thanks to the bounds of the right-hand side due to (3.9)–(3.10)) and using (3.13), we find that

$$\forall\,\varphi\in C_c^\infty((0,T)),\ \forall\,\boldsymbol{\varphi}\in H_{\mathrm{div},0}(\Omega),\ \int_0^T\int_\Omega\varphi(t)(\widetilde{G}\cdot\boldsymbol{\varphi}+u\ \operatorname{div}\boldsymbol{\varphi})\,\mathrm{d}x\,\mathrm{d}t=0.$$

This shows that $u\in L^2(0,T;H^1(\Omega))$ and that $\widetilde{G}(x,t)=\nabla u(x,t)$ for a.e. $(x,t)\in\Omega\times(0,T)$.

Let us now prove that u is a weak solution to (1.1)–(1.3) in the sense of Definition 2.1.

Let $\varphi\in C_c^\infty([0,T))$, and $w\in H^1(\Omega)$ be given. We denote by

$$w_m=\operatorname*{arg\,min}_{v\in X_{\mathcal{D}_m}}\bigl(\|\Pi_{\mathcal{D}_m}v-w\|_{L^2(\Omega)}^2+\|\nabla_{\mathcal{D}_m}v-\nabla w\|_{L^2(\Omega)^d}^2\bigr)^{1/2}.$$

Using (3.12), we have that $\Pi_{\mathcal{D}_m}w_m$ converges to w in $L^2(\Omega)$ and that $\nabla_{\mathcal{D}_m}w_m$ converges to ∇w in $L^2(\Omega)^d$. Then we set $v^n=\varphi((n-1)\tau)w_m$ in (3.7), and denote by $\varphi_m(t)$ the value $\varphi((n-1)\tau)$ for all $t\in((n-1)\tau,n\tau]$. We get $T_1^m+T_2^m=T_3^m$, with

$$T_1^m=\int_0^T\int_\Omega\delta_{\tau_m}u\,\Pi_{\mathcal{D}_m}w_m\varphi_m(t)\,\mathrm{d}x\,\mathrm{d}t,$$

$$T_2^m=\int_0^T\varphi_m(t)\int_\Omega G_{\mathcal{D}_m,\tau_m}(\Pi_{\mathcal{D}_m,\tau_m}u,x,t)\nabla_{\mathcal{D}_m,\tau_m}u\cdot\nabla_{\mathcal{D}_m}w_m\,\mathrm{d}x\,\mathrm{d}t,$$

and

$$T_3^m=\int_0^T\varphi_m(t)\int_\Omega r\,\Pi_{\mathcal{D}_m}w_m\,\mathrm{d}x\,\mathrm{d}t.$$

We can rewrite T_1^m as

$$T_1^m = -\int_\Omega u_{\rm ini}\Pi_{\mathcal{D}_m} w_m\varphi(0)\,\mathrm{d}x - \sum_{n=1}^{N_T}\int_\Omega \Pi_{\mathcal{D}_m}u^n\,\Pi_{\mathcal{D}_m}w_m(\varphi(n\tau)-\varphi((n-1)\tau))\,\mathrm{d}x\,\mathrm{d}t,$$

which gives

$$T_1^m = -\int_\Omega u_{\rm ini}\Pi_{\mathcal{D}_m} w_m\varphi(0)\,\mathrm{d}x - \int_0^T\int_\Omega \Pi_{\mathcal{D}_m,\tau_m}u\,\Pi_{\mathcal{D}_m}w_m\varphi_t(t)\,\mathrm{d}x\,\mathrm{d}t.$$

Hence, we get that

$$\lim_{m\to\infty} T_1^m = -\int_\Omega u_{\rm ini}w\ \varphi(0)\,\mathrm{d}x - \int_0^T\int_\Omega u\ w_m\varphi_t(t)\,\mathrm{d}x\,\mathrm{d}t.$$

Thanks to assumption (3.8), we have, for a.e. $(x,t)\in\Omega\times(0,T)$:

$$\begin{aligned}&|G_{\mathcal{D}_m,\tau_m}(\Pi_{\mathcal{D}_m,\tau_m}u,x,t) - G(u,x,t)|\\ &\qquad\leqslant C_{\mathcal{D}_m,\tau_m}\|\Pi_{\mathcal{D}_m,\tau_m}u(\cdot,t)\|_{L^2(\Omega)} + |G(\Pi_{\mathcal{D}_m,\tau_m}u,x,t) - G(u,x,t)|.\end{aligned}$$

Thanks to the assumption that $C_{\mathcal{D}_m,\tau_m}$ tends to 0 as $m\to\infty$, and thanks to the convergence of $\Pi_{\mathcal{D}_m,\tau_m}u(\cdot,t)$ to $u(\cdot,t)$ in $L^2(\Omega)$ for a.e. $t\in(0,T)$, we obtain that $G_{\mathcal{D}_m,\tau_m}(\Pi_{\mathcal{D}_m,\tau_m}u,x,t)$ converges to $G(u,x,t)$ for a.e. $(x,t)\in\Omega\times(0,T)$. Noticing that

$$\begin{aligned}&\int_\Omega G_{\mathcal{D}_m,\tau_m}(\Pi_{\mathcal{D}_m,\tau_m}u,x,t)\nabla_{\mathcal{D}_m,\tau_m}u\cdot\nabla_{\mathcal{D}_m}w_m\,\mathrm{d}x\\ &\qquad= \int_\Omega (G_{\mathcal{D}_m,\tau_m}(\Pi_{\mathcal{D}_m,\tau_m}u,x,t) - G(u,x,t))\nabla_{\mathcal{D}_m,\tau_m}u\cdot\nabla_{\mathcal{D}_m}w_m\,\mathrm{d}x\\ &\qquad\quad+\int_\Omega G(u,x,t)\nabla_{\mathcal{D}_m,\tau_m}u\cdot\nabla_{\mathcal{D}_m}w_m\,\mathrm{d}x,\end{aligned}$$

we get by dominated convergence for the first term and weak-strong convergence for the second term that

$$\lim_{m\to\infty} T_2^m = \int_0^T\varphi(t)\int_\Omega G(u,x,t)\nabla u\cdot\nabla w\,\mathrm{d}x\,\mathrm{d}t.$$

Finally, we also have

$$\lim_{m\to\infty} T_3^m = \int_0^T\varphi(t)\int_\Omega r\ w\,\mathrm{d}x\,\mathrm{d}t.$$

This achieves the proof that u is a weak solution to (1.1)–(1.3) in the sense of Definition 2.1. □

Theorem 3.2. *Under the hypotheses of Theorem* 3.1, *let* $(\mathcal{D}_m, \tau_m)_{m\in\mathbb{N}}$ *be a subsequence satisfying the properties stated in the conclusions of Theorem* 3.1. *Then* $\Pi_{\mathcal{D}_m,\tau_m} u_m(\cdot,t)$ *tends to* $u(t)$ *in* $L^2(\Omega)$ *for all* $t\in[0,T]$, *and* $\nabla_{\mathcal{D}_m} u_{\mathcal{D}_m,\tau_m}$ *tends to* ∇u *in* $L^2(\Omega\times(0,T))^d$. *In the case that* u *is unique, the whole sequence converges in the same sense.*

P r o o f. Let $w\in H^1(\Omega)$ and let

$$w_m = \operatorname*{arg\,min}_{v\in X_{\mathcal{D}_m}} (\|\Pi_{\mathcal{D}_m} v - w\|^2_{L^2(\Omega)} + \|\nabla_{\mathcal{D}_m} v - \nabla w\|^2_{L^2(\Omega)^d})^{1/2}.$$

Let us consider, for $s\leqslant t\in[0,T]$,

$$B(s,t) = \int_\Omega (\Pi_{\mathcal{D}_m,\tau_m} u_m(x,t) - \Pi_{\mathcal{D}_m,\tau_m} u_m(x,s)) \Pi_{\mathcal{D}_m} w_m(x)\,\mathrm{d}x.$$

We find that

$$\begin{aligned} B(s,t) &= \int_{(\nu(t)-1)\tau}^{\nu(t+s)\tau} \int_\Omega \delta_{\tau_m} u_m \Pi_{\mathcal{D}_m} w_m(x)\,\mathrm{d}x \\ &= \int_{(\nu(t)-1)\tau}^{\nu(t+s)\tau} \int_\Omega (r\Pi_{\mathcal{D}_m} w_m - G_{\mathcal{D}_m,\tau_m}(\Pi_{\mathcal{D}_m,\tau_m} u_m, x, t)\nabla_{\mathcal{D}_m,\tau_m} u\cdot\nabla_{\mathcal{D}_m} w_m)\,\mathrm{d}x\,\mathrm{d}t. \end{aligned}$$

Thanks to the Cauchy-Schwarz inequality, we get the existence of C_4, independent of m and w, such that

$$B(s,t)\leqslant(\nu(t+s)\tau-(\nu(t)-1)\tau)^{1/2} C_4\|w_m\|_{\mathcal{D}_m} \leqslant (t-s+2\tau_m)^{1/2} C_4\|w_m\|_{\mathcal{D}_m}.$$

This continuity property is sufficient to apply Theorem 6.1 (given in the Appendix), proving that for all $t\in[0,T]$, $\Pi_{\mathcal{D}_m,\tau_m} u_m(t)$ tends to $u(t)$ for the weak topology of $L^2(\Omega)$. In the same way as in the proof of Lemma 3.1, we have the property, for a given $t_0\in[0,T]$ (dropping the indices m),

(3.14)
$$\begin{aligned} \int_\Omega \left(\frac{1}{2}(\Pi_{\mathcal{D},\tau} u(x,t_0)^2 - u_{\mathrm{ini}}(x)^2) + \int_0^{\nu(t_0)\tau} G_{\mathcal{D},\tau}(\Pi_{\mathcal{D},\tau} u, x, t)\nabla_{\mathcal{D},\tau} u\cdot\nabla_{\mathcal{D},\tau} u\,\mathrm{d}t\right)\mathrm{d}x \\ \leqslant \int_0^{\nu(t_0)\tau}\int_\Omega r(x,t)\Pi_{\mathcal{D},\tau} u(x,t)\,\mathrm{d}x\,\mathrm{d}t. \end{aligned}$$

Passing to the limit in the above inequality, we arrive at

$$\begin{aligned} \limsup_{m\to\infty} \left(\frac{1}{2}\int_\Omega \Pi_{\mathcal{D},\tau} u(x,t_0)^2 + \int_0^{\nu(t_0)\tau} G_{\mathcal{D},\tau}(\Pi_{\mathcal{D},\tau} u, x, t)\nabla_{\mathcal{D},\tau} u\cdot\nabla_{\mathcal{D},\tau} u\,\mathrm{d}t\right)\mathrm{d}x \\ \leqslant \frac{1}{2}\int_\Omega u_{\mathrm{ini}}(x)^2\,\mathrm{d}x + \int_0^{t_0}\int_\Omega r(x,t)u(x,t)\,\mathrm{d}x\,\mathrm{d}t. \end{aligned}$$

Since u satisfies (2.3), we have

$$\frac{1}{2}\int_\Omega u(x,t_0)^2\,\mathrm{d}x + \int_0^{t_0}\!\!\int_\Omega G(u,x,t)\nabla u\cdot\nabla u\,\mathrm{d}x\,\mathrm{d}t = \frac{1}{2}\int_\Omega (u_{\mathrm{ini}})^2\,\mathrm{d}x + \int_0^{t_0}\!\!\int_\Omega r\ u\,\mathrm{d}x\,\mathrm{d}t.$$

The weak convergence of $\Pi_{\mathcal{D},\tau}u(\cdot,t_0)$ to $u(\cdot,t_0)$ and of $\nabla_{\mathcal{D},\tau}u$ to ∇u implies that

$$\liminf_{m\to\infty}\frac{1}{2}\int_\Omega \Pi_{\mathcal{D},\tau}u(x,t_0)^2 \geqslant \frac{1}{2}\int_\Omega u(x,t_0)^2\,\mathrm{d}x,$$

$$\liminf_{m\to\infty}\int_0^{\nu(t_0)\tau} G_{\mathcal{D},\tau}(\Pi_{\mathcal{D},\tau}u,x,t)\nabla_{\mathcal{D},\tau}u\cdot\nabla_{\mathcal{D},\tau}u\,\mathrm{d}t\,\mathrm{d}x \geqslant \int_0^{t_0}\!\!\int_\Omega G(u,x,t)\nabla u\cdot\nabla u\,\mathrm{d}x\,\mathrm{d}t.$$

Therefore, we obtain

$$\lim_{m\to\infty}\frac{1}{2}\int_\Omega \Pi_{\mathcal{D},\tau}u(x,t_0)^2 = \frac{1}{2}\int_\Omega u(x,t_0)^2\,\mathrm{d}x,$$

$$\lim_{m\to\infty}\int_0^{\nu(t_0)\tau} G_{\mathcal{D},\tau}(\Pi_{\mathcal{D},\tau}u,x,t)\nabla_{\mathcal{D},\tau}u\cdot\nabla_{\mathcal{D},\tau}u\,\mathrm{d}t\,\mathrm{d}x = \int_0^{t_0}\!\!\int_\Omega G(u,x,t)\nabla u\cdot\nabla u\,\mathrm{d}x\,\mathrm{d}t,$$

hence concluding the proof of the strong convergence. □

4. A particular gradient scheme

In order to describe the scheme, we now introduce some notation for the space discretization. Let now Ω be a rectangular domain as is standard in image processing.

(1) A *rectangular discretization* of Ω is defined by the increasing sequences $a_i = x_0^{(i)} < x_1^{(i)} < \ldots < x_{n^{(i)}}^{(i)} = b_i$, $i = 1,\ldots,d$.

(2) We denote by

$$\mathcal{M} = \{(x_{i^{(1)}}^{(1)}, x_{i^{(1)}+1}^{(1)}) \times \ldots \times (x_{i^{(d)}}^{(d)}, x_{i^{(d)}+1}^{(d)}),\\ 0 \leqslant i^{(1)} < n^{(1)},\ \ldots,\ 0 \leqslant i^{(d)} < n^{(d)}\}$$

the set of control volumes. The elements of $\mathcal{M}$ are denoted $p, q, \ldots$ We denote by $\boldsymbol{x}_p$ the center of p. For any $p \in \mathcal{M}$, let $\partial p = \overline{p} \setminus p$ be the boundary of p; let $|p| > 0$ denote the measure of p, h_p denote the diameter of p and $h_{\mathcal{D}}$ denote the maximum value of $(h_p)_{p\in\mathcal{M}}$.

(3) We denote by E_p the set of all faces of $p \in \mathcal{M}$ (it has $2d$ elements), by E the union of all E_p, and for every $\sigma \in E$, we denote by $|\sigma|$ its $(d-1)$-dimensional measure. For any $\sigma \in E$, we define the set $\mathcal{M}_\sigma = \{p \in \mathcal{M}, \sigma \in E_p\}$ (which has therefore one or two elements) and by $\boldsymbol{x}_\sigma$ we denote the center of σ. We then denote by $d_{p\sigma} = |\boldsymbol{x}_\sigma - \boldsymbol{x}_p|$ the orthogonal distance between $\boldsymbol{x}_p$ and $\sigma \in E_p$ and by $\mathbf{n}_{p,\sigma}$ the normal vector to σ, outward to p.

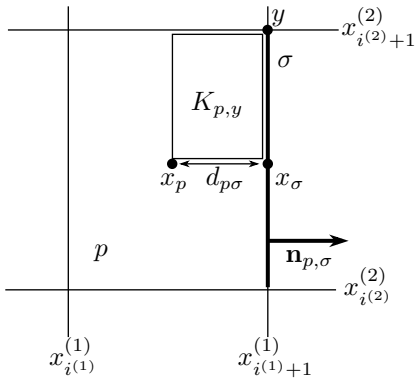

Figure 1. Notation for the meshes.

(4) We denote by $\mathcal{V}_p$ the set of all vertices of $p \in \mathcal{M}$ (it has 2^d elements), by $\mathcal{V}$ the union of all $\mathcal{V}_p$, $p \in \mathcal{M}$. For $y \in \mathcal{V}_p$, we denote by $K_{p,y}$ the rectangle whose faces are parallel to those of p, and whose set of vertices contains $\boldsymbol{x}_p$ and y. We denote by $\mathcal{V}_\sigma$ the set of all vertices of $\sigma \in E$ (it has 2^{d-1} elements), and by $E_{p,y}$ the set of all $\sigma \in E_p$ such that $y \in \mathcal{V}_\sigma$ (it has d elements).

(5) We define the set $X_{\mathcal{D}}$ of all $u = ((u_p)_{p\in\mathcal{M}}, (u_{\sigma,y})_{\sigma\in E, y\in\mathcal{V}_\sigma})$.

(6) We denote, for all $u \in X_{\mathcal{D}}$, by $\Pi_{\mathcal{D}} u \in L^2(\Omega)$ the function defined by the constant value u_p a.e. in $p \in \mathcal{M}$.

(7) For $u \in X_{\mathcal{D}}$, $p \in \mathcal{M}$ and $y \in \mathcal{V}_p$, we denote by

$$\nabla_{p,y} u = \frac{2}{|p|} \sum_{\sigma\in E_{p,y}} |\sigma|(u_{\sigma,y} - u_p)\mathbf{n}_{p,\sigma} = \sum_{\sigma\in E_{p,y}} \frac{u_{\sigma,y} - u_p}{d_{p\sigma}} \mathbf{n}_{p,\sigma}, \tag{4.1}$$

and by $\nabla_{\mathcal{D}} u$ the function defined a.e. on Ω by $\nabla_{p,y} u$ on $K_{p,y}$.

We then have the following result.

Lemma 4.1. *Let $\Omega = (a_1, b_1) \times \ldots \times (a_d, b_d)$ be an open rectangle in $\mathbb{R}^d$. Let $\mathcal{D} = (X_{\mathcal{D}}, \Pi_{\mathcal{D}}, \nabla_{\mathcal{D}})$ be a rectangular discretization as described above. Then $\mathcal{D}$ is an approximate gradient discretization in the sense of Definition 3.1, such that under the regularity condition $(x^{(j)}_{i^{(j)}+1} - x^{(j)}_{i^{(j)}})/(x^{(k)}_{i^{(k)}+1} - x^{(k)}_{i^{(k)}}) \leqslant C$, $j, k = 1, 2, \ldots, d$, we get the existence of $\widetilde{T}\colon \mathbb{R}^d \to \mathbb{R}^+$ with $\lim_{|\xi|\to 0} \widetilde{T}(\xi) = 0$ such that $T_{\mathcal{D}} \leqslant \widetilde{T}$ independently of $h_{\mathcal{D}}$, and that*

$$\forall\, \varphi \in H^1(\Omega), \quad \lim_{h_{\mathcal{D}}\to 0} S_{\mathcal{D}}(\varphi) = 0, \tag{4.2}$$

and

$$\forall\, \boldsymbol{\varphi} \in H_{\mathrm{div},0}(\Omega), \quad \lim_{h_{\mathcal{D}}\to 0} W_{\mathcal{D}}(\boldsymbol{\varphi}) = 0. \tag{4.3}$$

P r o o f. Let us recall the result, proved in [12]: for such a rectangular discretization $\mathcal{D}$, the expression $\|u\|_{\mathcal{D}}$, defined by

$$\|u\|_{\mathcal{D}}^2 = \sum_{p\in\mathcal{M}} |p|\, u_p^2 + \sum_{p\in\mathcal{M}} \sum_{\sigma\in E_p} \sum_{y\in\mathcal{V}_\sigma} \frac{|\sigma|}{d_{p\sigma}} (u_{\sigma,y} - u_p)^2 \quad \forall\, u \in X_{\mathcal{D}},$$

is a norm on $X_{\mathcal{D}}$ such that (4.2) holds, where C only depends on the bound on θ. The limit conformity property (4.3) is proved in the same way as in [12]. We then remark that $\|u\|_{\mathcal{D}}^2$ controls the semi-norm $|\cdot|_{1,\mathcal{T}}$ as defined in [11], Definition 10.2, page 795. We can therefore follow the proof of [11], Theorem 10.3, page 810 using the discrete trace inequality [11], Lemma 10.5, page 807 in the case of the homogeneous Neumann boundary conditions, which proves the existence of T as given in this statement (hence proceeding in the same way as in [9]). □

R e m a r k 4.1. The equations obtained, for a given $y \in \mathcal{V}$, defining $v \in X_{\mathcal{D}}$ for a given $\sigma \in E_y$ by $v_{\sigma,y} = 1$ and all other degrees of freedom null, constitute a local invertible linear system, allowing for expressing all $(u_{\sigma,y})_{\sigma\in E_y}$ with respect to all $(u_{p,y})_{p\in\mathcal{M}_y}$. This leads to a nine-point stencil on rectangular meshes in 2D, and a 27-point stencil in 3D (this property is the basis of the MPFA O-scheme [1]).

5. Numerical experiments

E x a m p l e 5.1. This example is devoted to a 1D illustration of the time-delayed regularization of the Perona-Malik equation, as described by (1.13) in the introduction of this paper. We consider the case $\Omega = (0,1)$, $u_{\rm ini}(x) = 2x$, and $\alpha = 1/101$ in (1.13). We then apply the scheme presented in Section 4 (it then resumes to a standard 3-point finite volume scheme), using various values of $\overline{t}$. We then show in Figure 5 the results computed at the final time $T = 50$, for $h = 1/500$ for $\overline{t} = 0.2$ and $\overline{t} = 0.5$ and $\tau = 0.01$. We see that although the problem is regularized, the numerical solution shows discontinuities resulting from the ill-posedness of the Perona-Malik equation. Turning to the values $\overline{t} = 1$ and $\overline{t} = 5$, with $\tau = 0.1$, we observe in Figure 5 that the regularity of the numerical solution is significantly increased.

E x a m p l e 5.2. In this example we present results of numerical computations for the regularized Perona-Malik equation in $2D$, where the regularization is again of the type (1.13). We assume that $\Omega = [0,1]\times[0,1]$, and we chose the right hand side r such that $u(x,y,t) = C((x^2+y^2)/2 - (x^3+y^3)/3)t$ is an exact strong solution of the problem (1.1)–(1.3). Two test cases, with different time delays $\bar{t}$, final times T and coefficients C, are presented. The errors in $L_2((0,T),L_2(\Omega))$ and $L_\infty((0,T),L_2(\Omega))$

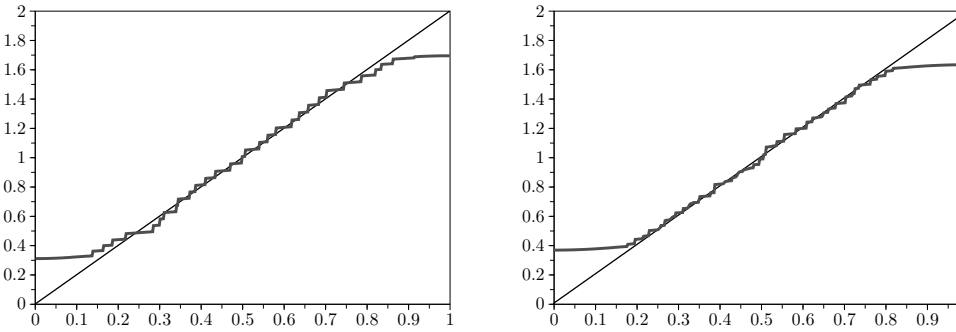

Figure 2. $\bar{t} = 0.2$, $\tau = 0.01$ (left), $\bar{t} = 0.5$, $\tau = 0.01$ (right).

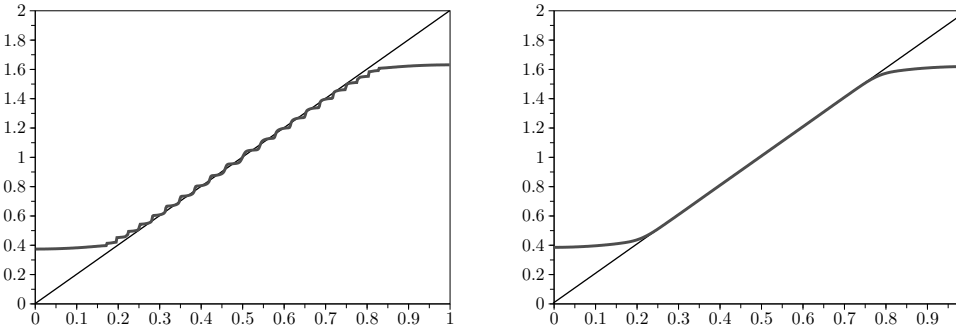

Figure 3. $\bar{t} = 1$, $\tau = 0.01$ (left), $\bar{t} = 5$, $\tau = 0.1$ (right).

for the solution u (denoted by E_2, E_∞) and for its gradient (denoted by EG_2, EG_∞) together with the experimental order of convergence (EOC) are presented in Table 1 for the case $\bar{t} = 0.0625$, $T = 0.625$ and $C = 1$, and in Table 2 for the case $\bar{t} = 0.625$, $T = 6.25$ and $C = \bar{t}/T = 0.1$. These numerical results indicate that the method is second order accurate, both in solution and gradient approximation.

n	τ	E_2	EOC	E_∞	EOC	EG_2	EOC	EG_∞	EOC
4	0.0625	4.771e-4	–	1.022e-3	–	7.184e-3	–	1.450e-2	–
8	0.015625	1.172e-4	1.429	2.692e-4	1.925	1.707e-3	2.073	3.615e-3	2.004
16	0.00390625	2.913e-5	2.604	6.812e-5	1.982	4.213e-4	2.019	9.031e-4	2.001
32	0.0009765625	7.270e-6	2.002	1.708e-5	1.996	1.050e-4	2.004	2.257e-4	2.000
64	0.000244140625	1.815e-6	2.001	4.273e-6	1.999	2.624e-5	2.000	5.643e-5	1.999

Table 1. Example 5.2, $\bar{t} = 0.0625$, $T = 0.625$, $C = 1$.

E x a m p l e 5.3. Image filtering by the time-delayed Perona-Malik model. In this experiment, we show the results obtained when filtering a noisy image, using the time-delay regularization of the Perona-Malik equation as given by (1.13). The original

n	τ	E_2	EOC	E_∞	EOC	EG_2	EOC	EG_∞	EOC
4	0.0625	1.778e-3	–	1.209e-3	–	2.032e-2	–	1.400e-2	–
8	0.015625	4.594e-4	1.952	3.173e-4	1.930	5.034e-3	2.031	3.478e-3	2.001
16	0.00390625	1.158e-4	1.988	8.021e-5	1.984	1.255e-3	2.004	8.680e-4	2.002
32	0.0009765625	2.898e-5	1.998	2.011e-5	1.996	3.137e-4	2.000	2.169e-4	2.001
64	0.000244140625	7.248e-6	1.999	5.030e-6	1.999	7.842e-5	2.000	5.422e-5	2.000

Table 2. Example 5.2, $\bar{t} = 0.625$, $T = 6.25$, $C = \frac{\bar{t}}{T} = 0.1$.

image (Figure 5 left top) is damaged by 40 percent additive noise (Figure 5 right top). In the bottom row of Figure 5 we present the 1st, 10th and 25th denoising steps which show a correct reconstruction of the original figure. The following parameters are used in the computations: $n^{(1)} = n^{(2)} = 200$, $h = 0.1$, $\tau = 0.1$, $\bar{t} = 0.1$. In the nonlinear function g defined by (1.6), we use the value of parameter $K = 100$. We observe that the denoised image does not show any significant alteration after 25 steps, compared to the initial one.

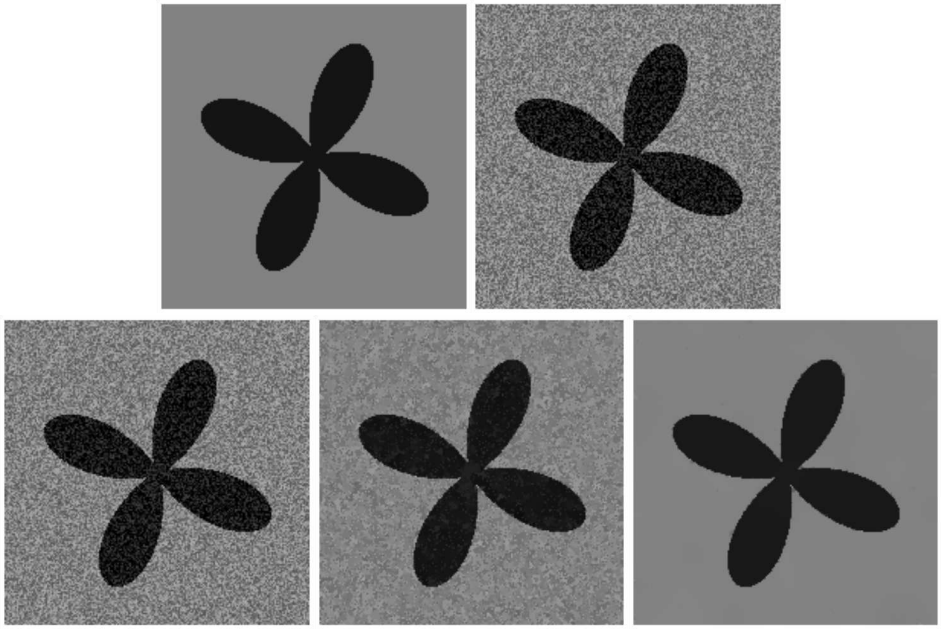

Figure 4. Example 5.3, the original image (left top), the noisy image (right top) and the results after 1, 10, 25 time steps (bottom, from left to right) of filtering.

E x a m p l e 5.4. Image filtering by the nonlinear tensor diffusion. In this example we present image denoising by the so-called coherence enhancing tensor diffusion [21], that means the case, where the diffusion coefficient is given by a matrix. The math-

ematical model is given in the introduction of this paper by (1.9)–(1.10) and (1.11)–(1.12). In this experiment we use the following parameters: $n^{(1)} = n^{(2)} = 250$, $h = 0.001$, $\bar{t} = 0.000001$, $\tau = 0.000001$. The chosen parameters in the convolution operators are defined by $\sigma = 0.0001$ and $\varrho = 0.01$, and the parameters in (1.11) are $\alpha = 0.0001$, $C = 1$. The convolution is realized in both cases by computing heat equation for time σ and ϱ, respectively, in similar way as in [18]. The scheme uses explicit values for G, which leads to the definition of a semi-implicit scheme for the nonlinear tensor diffusion model as in [9], [8]. In Figure 5, one can see the original image with three crackling lines, and the results after 2 and 5 time steps, showing that the coherence of the line structures has been improved.

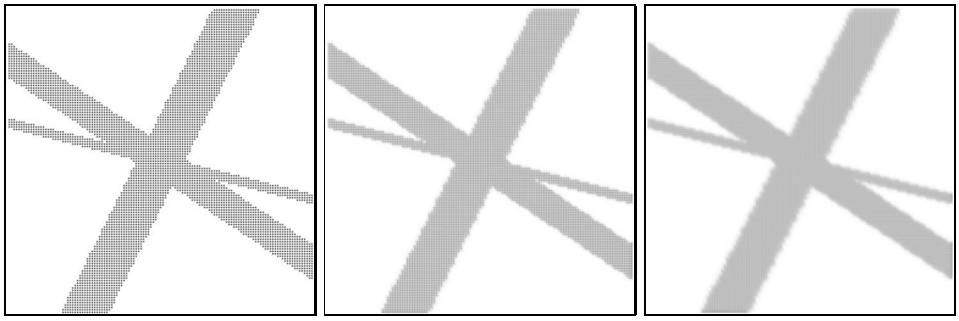

Figure 5. Example 5.4, the original image (left), the results after 2 (middle) and 5 (right) time steps.

6. Conclusion

Gradient schemes have recently been shown to be efficient for the discretization of elliptic problems and steady state coupled problems. The present paper shows that the mathematical framework of the Gradient Scheme also applies to the discrete analysis of parabolic problems involved in some practical applications. The particular gradient scheme used in this paper for image processing applications leads to a 9-point stencil finite volume type scheme, which is unconditionally coercive and convergent. In the image processing problem under consideration, structural (pixel, voxel) grids are mainly used; however, other important data processing applications [7] rely on general triangulated grids (also on surfaces), for which the gradient scheme may still be used. Its use in further applications will be studied in future works, as well as its comparison with other schemes [19], [9].

Appendix

Lemma 6.1. *Let $T > 0$ be given, and let $\tau = T/N_T$, for $N_T \in \mathbb{N}^\star$. For all $t \in [0,T]$, we denote by $\nu(t)$ the element $n \in \mathbb{N}$ such that $t \in ((n-1)\tau, n\tau])$. Let $(a^n)_{n=1,\dots,N_T}$ be a family of nonnegative real values. Then*

$$\int_0^{T-\eta} \sum_{n=\nu(t)}^{\nu(t+\eta)} (\tau a^n)\,\mathrm{d}t = \eta \sum_{n=1}^{N_T} (\tau a^n) \quad \forall\, \eta \in (0,T) \tag{6.1}$$

and

$$\int_0^{T-\eta} \Bigg(\sum_{n=\nu(t)+1}^{\nu(t+\eta)} \tau \Bigg) a^{\nu(t+s)}\,\mathrm{d}t \leqslant \eta \sum_{n=1}^{N_T} (\tau a^n) \quad \forall\, \eta \in (0,T),\ \forall\, s \in (0,\eta). \tag{6.2}$$

The proof of the above lemma follows that of [11], Proof of Lemma 18.6, page 855.

Theorem 6.1. *Let Ω be an open bounded subset of $\mathbb{R}^2$, $a < b \in \mathbb{R}$ and $(u_m)_{m\in\mathbb{N}}$ be a sequence of functions from $[a,b]$ to $L^2(\Omega)$, such that there exists $C_1 > 0$ with*

$$\|u_m(t)\|_{L^2(\Omega)} \leqslant C_1 \quad \forall\, m \in \mathbb{N},\ \forall\, t \in [a,b]. \tag{6.3}$$

We also assume that there exists $(\tau_m)_{m\in\mathbb{N}}$ with $\tau_m \geqslant 0$ and $\lim\limits_{m\to\infty} \tau_m = 0$ and a dense subset R of $L^2(\Omega)$ such that for all $\varphi \in R$, there exists $C_\varphi > 0$ such that

$$|\langle u_m(t_2) - u_m(t_1), \varphi\rangle_{L^2(\Omega),L^2(\Omega)}| \leqslant C_\varphi (t_2 - t_1 + 2\tau_m)^{1/2} \quad \forall\, m \in \mathbb{N},\ \forall\, a \leqslant t_1 \leqslant t_2 \leqslant b. \tag{6.4}$$

Then there exists $u \in L^\infty(a,b;L^2(\Omega))$ with $u \in C_w([a,b],L^2(\Omega))$ (where we denote by $C_w([a,b],L^2(\Omega))$ the set of functions from $[a,b]$ to $L^2(\Omega)$, continuous for the weak topology of $L^2(\Omega)$) and a subsequence of $(u_m)_{m\in\mathbb{N}}$, again denoted by $(u_m)_{m\in\mathbb{N}}$, such that for all $t \in [a,b]$, $u_m(t)$ converges to $u(t)$ for the weak topology of $L^2(\Omega)$.

P r o o f. The proof follows that of Ascoli's theorem, and we provide it only for completeness (a similar proof is also provided in [16] in the framework of the weak star topology of Radon measures). Let $(t_p)_{p\in\mathbb{N}}$ be a sequence of real numbers, dense in $[a,b]$. Due to (6.3), for each $p \in \mathbb{N}$, we may extract from $(u_m(t_p))_{m\in\mathbb{N}}$ a subsequence which is convergent to some element of $L^2(\Omega)$ for the weak topology of $L^2(\Omega)$. Using the diagonal method, we can choose a subsequence, again denoted by $(u_m)_{m\in\mathbb{N}}$, such that $(u_m(t_p))_{m\in\mathbb{N}}$ is weakly convergent for all $p \in \mathbb{N}$. For any $t \in [a,b]$ and $v \in L^2(\Omega)$,

we then prove that the sequence $(\langle u_m(t), v\rangle_{L^2(\Omega),L^2(\Omega)})_{m\in\mathbb{N}}$ is a Cauchy sequence. Indeed, let $\varepsilon > 0$ be given. We first choose $\varphi \in R$ such that $\|\varphi - v\|_{L^2(\Omega)} \leqslant \varepsilon$. Then, we choose $p \in \mathbb{N}$ such that $|t - t_p| \leqslant (\varepsilon/C_\varphi)^2$. Since $(\langle u_m(t_p), \varphi\rangle_{L^2(\Omega),L^2(\Omega)})_{m\in\mathbb{N}}$ is a Cauchy sequence, we choose $n_0 \in \mathbb{N}$ such that for $k, l \geqslant n_0$,

$$|\langle u_k(t_p) - u_l(t_p), \varphi\rangle_{L^2(\Omega),L^2(\Omega)}| \leqslant \varepsilon,$$

and such that $\tau_k, \tau_l \leqslant (\varepsilon/C_\varphi)^2$. We then get, using (6.4),

$$|\langle u_k(t) - u_l(t), \varphi\rangle_{L^2(\Omega),L^2(\Omega)}| \leqslant C_\varphi((|t - t_p| + 2\tau_k)^{1/2} + (|t - t_p| + 2\tau_l)^{1/2}) + \varepsilon,$$

which gives

$$|\langle u_k(t) - u_l(t), \varphi\rangle_{L^2(\Omega),L^2(\Omega)}| \leqslant 2\ 3^{1/2}\varepsilon + \varepsilon.$$

We then get, using (6.3),

$$|\langle u_k(t) - u_l(t), v\rangle_{L^2(\Omega),L^2(\Omega)}| \leqslant 2C_1\varepsilon + 2\ 3^{1/2}\varepsilon + \varepsilon.$$

This proves that the sequence $(\langle u_m(t), v\rangle_{L^2(\Omega),L^2(\Omega)})_{m\in\mathbb{N}}$ converges. Since

$$|\langle u_m(t), v\rangle_{L^2(\Omega),L^2(\Omega)}| \leqslant C_1\|v\|_{L^2(\Omega)},$$

we get the existence of $u(t) \in L^2(\Omega)$ such that $(u_m(t))_{m\in\mathbb{N}}$ converges to $u(t)$ for the weak topology of $L^2(\Omega)$. Then $u \in C_w([a, b], L^2(\Omega))$ is obtained by passing to the limit $m \to \infty$ in (6.4), and by using the density of R in $L^2(\Omega)$. □

References

[1] *I. Aavatsmark, T. Barkve, Ø. Bøe, T. Mannseth*: Discretization on non-orthogonal, quadrilateral grids for inhomogeneous, anisotropic media. J. Comput. Phys. *127* (1996), 2–14. zbl

[2] *H. Amann*: Time-delayed Perona-Malik type problems. Acta Math. Univ. Comen., New Ser. *76* (2007), 15–38. zbl MR

[3] *S. Bartels, A. Prohl*: Stable discretization of scalar and constrained vectorial Perona-Malik equation. Interfaces Free Bound. *9* (2007), 431–453. zbl MR

[4] *G. Bellettini, M. Novaga, M. Paolini, C. Tornese*: Convergence of discrete schemes for the Perona-Malik equation. J. Differ. Equations *245* (2008), 892–924. zbl MR

[5] *C. Cancès, T. Gallouët*: On the time continuity of entropy solutions. J. Evol. Equ. *11* (2011), 43–55. zbl MR

[6] *F. Catté, P.-L. Lions, J.-M. Morel, T. Coll*: Image selective smoothing and edge detection by nonlinear diffusion. SIAM J. Numer. Anal. *29* (1992), 182–193. zbl MR

[7] *R. Čunderlík, K. Mikula, M. Tunega*: Nonlinear diffusion filtering of data on the Earth's surface. J. Geod. *87* (2013), 143–160.

[8] *O. Drblíková, A. Handlovičová, K. Mikula*: Error estimates of the finite volume scheme for the nonlinear tensor-driven anisotropic diffusion. Appl. Numer. Math. *59* (2009), 2548–2570. zbl MR
[9] *O. Drblíková, K. Mikula*: Convergence analysis of finite volume scheme for nonlinear tensor anisotropic diffusion in image processing. SIAM J. Numer. Anal. *46* (2007), 37–60. zbl MR
[10] *J. Droniou, R. Eymard, T. Gallouët, R. Herbin*: A unified approach to mimetic finite difference, hybrid finite volume and mixed finite volume methods. Math. Models Methods Appl. Sci. *20* (2010), 265–295. zbl MR
[11] *R. Eymard, T. Gallouët, R. Herbin*: Finite volume methods. Handbook of numerical analysis. Vol. 7: Solution of equations in $\mathbb{R}^n$ (Part 3) (P. G. Ciarlet et al., eds.). Techniques of scientific computing (Part 3), North Holland/Elsevier, Amsterdam, 2000, pp. 713–1020. zbl MR
[12] *R. Eymard, T. Gallouët, R. Herbin*: Discretization of heterogeneous and anisotropic diffusion problems on general nonconforming meshes SUSHI: a scheme using stabilization and hybrid interfaces. IMA J. Numer. Anal. *30* (2010), 1009–1043. zbl MR
[13] *R. Eymard, C. Guichard, R. Herbin*: Small-stencil 3D schemes for diffusive flows in porous media. ESAIM, Math. Model. Numer. Anal. *46* (2012), 265–290. zbl MR
[14] *R. Eymard, R. Herbin*: Gradient scheme approximations for diffusion problems. Finite Volumes for Complex Applications 6: Problems and Perspectives. Vol. 1, 2. Conf. Proc. (J. Fořt et al., eds.). Proceedings in Mathematics 4, Springer, Heidelberg, 2011, pp. 439–447. zbl MR
[15] *R. Eymard, R. Herbin, J. C. Latché*: Convergence analysis of a colocated finite volume scheme for the incompressible Navier-Stokes equations on general 2D or 3D meshes. SIAM J. Numer. Anal. *45* (2007), 1–36. zbl MR
[16] *R. Eymard, S. Mercier, A. Prignet*: An implicit finite volume scheme for a scalar hyperbolic problem with measure data related to piecewise deterministic Markov processes. J. Comput. Appl. Math. *222* (2008), 293–323. zbl MR
[17] *A. Handlovičová, Z. Krivá*: Error estimates for finite volume scheme for Perona-Malik equation. Acta Math. Univ. Comen., New Ser. *74* (2005), 79–94. zbl MR
[18] *A. Handlovičová, K. Mikula, F. Sgallari*: Semi-implicit complementary volume scheme for solving level set like equations in image processing and curve evolution. Numer. Math. *93* (2003), 675–695. zbl MR
[19] *K. Mikula, N. Ramarosy*: Semi-implicit finite volume scheme for solving nonlinear diffusion equations in image processing. Numer. Math. *89* (2001), 561–590. zbl MR
[20] *P. Perona, J. Malik*: Scale-space and edge detection using anisotropic diffusion. IEEE Trans. Pattern Anal. Mach. Intell. *12* (1990), 629–639.
[21] *J. Weickert*: Coherence-enhancing diffusion filtering. Int. J. Comput. Vis. *31* (1999), 111–127.

Authors' addresses: *R. Eymard*, Université Paris-Est, 5 boulevard Descartes, Cité Descartes, Champs-sur-Marne, 774 54 Marne-la-Vallée, Cedex 2, France e-mail: `robert.eymard@univ-mlv.fr`; *A. Handlovičová*, Slovak University of Technology, Department of Mathematics and Constructive Geometry, Radlinského 11, Bratislava, Slovakia, e-mail: `angela.handlovicova@stuba.sk`; *R. Herbin*, Centre de Mathématiques et Informatique (CMI), Aix-Marseille Université, Technopôle Château-Gombert, 39, rue F. Joliot Curie, 134 53 Marseille Cedex 13, France, e-mail: `raphaele.herbin@cmi.univ-mrs.fr`; *K. Mikula*, *O. Stašová*, Slovak University of Technology, Department of Mathematics and Constructive Geometry, Radlinského 11, Bratislava, Slovakia, e-mail: `mikula@math.sk`, `stasova@math.sk`.